Control of a hybrid electric vehicle with dual clutch transmission configurations during mode transition

Walid Elzaghir*

Department of Electrical and Computer Engineering,
University of Michigan-Dearborn,
Dearborn, MI 48128, USA
Email: wmel@umich.edu
*Corresponding author

Yi Zhang

Department of Mechanical Engineering,
University of Michigan-Dearborn,
Dearborn, MI 48128, USA
Email: anding@umich.edu

Narasimhamurthi Natarajan

Department of Electrical and Computer Engineering
University of Michigan-Dearborn,
Dearborn, MI 48128, USA
Email: nattu7@gmail.com

Frank Massey

Department of Mathematics,
University of Michigan-Dearborn,
Dearborn, MI 48128, USA
Email: fmassey@umich.edu

Chris Mi

Department of Electrical and Computer Engineering,
San Diego State University,
5500 Campanile Drive,
San Diego, CA 92182, USA
Email: mi@ieee.org

Hafiz Malik

Department of Electrical and Computer Engineering,
University of Michigan-Dearborn,
Dearborn, MI 48128, USA
Email: hafiz@umich.edu

Abstract: Mode transitions are significant events in the operation of a hybrid electric vehicle with dual clutch transmission (HDCT). Owing to the friction-induced discontinuity of the clutch torque, seamless transition is difficult to achieve. First, this paper presents mathematical equations for the nonlinear system. Then it presents the linearised model for the proposed system. The control objective of the model reference adaptive controller (MRAC) considered in this paper is to minimise fuel consumption and reduce torque interruption in a hybrid electric vehicle (HEV). The simulation and experimental results from an HDCT demonstrate that the MRAC achieves reduced torque interruption and less vehicle jerk compared to the conventional operation method, in addition to smooth and fast transition from pure electrical driving to hybrid driving.

Keywords: HEV; hybrid electric vehicle; HDCT; hybrid electric vehicle with dual clutch transmission; mode transition; MRAC; model reference adaptive control.

Reference to this paper should be made as follows: Elzaghir, W., Zhang, Y., Natarajan, N., Massey, F., Mi, C. and Malik, H. (2018) 'Control of a hybrid electric vehicle with dual clutch transmission configurations during mode transition', *Int. J. Electric and Hybrid Vehicles*, Vol. 10, No. 1, pp.1–25.

Biographical notes: Walid Elzaghir received his BS and the MS from the University of Michigan-Dearborn in 2004 and 2009, respectively, all in Electrical Engineering. He joined the ITT as Electronic Teacher in 2009 and He is currently a PhD student with the Department of Electrical Engineering.

Yi Zhang received his BS from Central South University, China, in 1982 and the MS and PhD from the University of Illinois at Chicago in 1986 and 1989, respectively, all in Mechanical Engineering. He joined the University of Michigan-Dearborn in 1992 and is currently an Associate Professor of Mechanical Engineering. His teaching and research interests are in the areas of gear design and manufacturing, theory of gearing, mechanical design, and vehicle powertrains. He has published more than 40 technical papers in gear design and power transmission areas. He is a Member of ASME.

Narasimhamurthi Natarajan graduated from Ramakrishna Mission High School Vivekananda Junior College and the Indian Institute of Technology all in Madras before coming to the US in 1974 and attending the University of California Berkley for his Master's and PhD degrees. He received his PhD at the age of 26 and after a year as Faculty at Washington University in St. Louis. He is an Associate Professor with the Department of Electrical Engineering, University of Michigan-Dearborn.

Frank Massey earned his Bachelor's degree in Mathematics from the University of California at Los Angeles and his PhD in Mathematics from the University of California at Berkeley. He joined the University of Michigan-Dearborn in 1978

after teaching for seven years at the University of Kentucky. His teaching and research interests are in applied mathematics with particular interest in probability and differential equations.

Chris Mi received the B.S.E.E. and M.S.E.E. degrees in Electrical Engineering from North-western Polytechnical University, Xi'an, China, and the PhD in Electrical Engineering from the University of Toronto, Toronto, Ontario, Canada. He is a Professor and Chair of Electrical and Computer Engineering at San Diego State University. Prior to that, he was a Professor at the University of Michigan, Dearborn, from 2001 to 2015, and he was with General Electric Company, Peterborough, Ontario, Canada. His research interests include electric drives, power electronics, electric machines, renewable-energy systems, and electrical and hybrid vehicles.

Hafiz Malik is an Associate Processor in the Electrical and Computer Engineering (ECE) Department at University of Michigan – Dearborn. His researches focus in cybersecurity, multimedia forensics, information security, wireless sensor networks. He has published more than 70 papers in leading journals, conferences, and workshops. He is serving as an Associate Editor for the *IEEE Transactions on Information Forensics and Security* since August 2014. He is also organising a special session on "Data Mining in Industrial Applications" within the IEEE Symposium Series on Computational Intelligence (IEEE SSCI) 2013. He is serving as vice chair of IEEE SEM, Chapter 16 since 2011.

1 Introduction

Hybrid electric vehicles with parallel architecture and dual clutch transmission (HDCT) are studied in this paper. These vehicles offer the flexibility of improving fuel economy and emissions without sacrificing safety and reliability. The durability and performance enhancements of HEVs have encouraged the development of the appropriate powertrain configurations and associated component resizing and control strategies.

A hybrid electric vehicle with dual clutch transmission (HDCT) typically consists of an internal combustion engine (ICE), an electric motor, and a dual clutch transmission (DCT), as shown in Figure 1. To make full use of the HDCT powertrain topology, frequent transitions between different modes are necessary to optimise the vehicle's operation (Waltermann, 1996). The torques produced by the ICE and the motor are combined at the transmission and the total torque is transferred to the wheels (Conlon, 2005). The DCTs have two input shafts. Therefore, by connecting an electric machine to one of the shafts, a hybrid dual clutch transmission can be obtained. The motor can also be made to work as a generator, thereby obtaining full hybrid functionality.

One special challenge in managing mode transition for the HDCT is to switch smoothly between the different modes, as the clutch friction torque introduces nonlinear dynamics to the powertrain and makes the clutch operation very complicated. If the torque lost by the system during mode transition is not carefully controlled, the lost torque may become discontinuous and abruptly change when the transition takes place. This discontinuity may result in an intense vehicle jerk and lead to unfavourable customer drivability perceptions. Given that the longitudinal dynamics of the vehicle are controlled by the motor torque solely in the motor-only driving mode, whereas in the combined driving mode they are controlled

by both the motor torque and the engine torque, one key function of the mode transition is to control the motor torque to cover all power lost in the hybrid system. For a seamless mode transition where no disturbance is introduced to the vehicle dynamics, the vehicle is expected to run as if it were still in the motor-only driving mode. This desired feature can be refined into the following control design objective: to coordinate the motor and the engine torques so that the vehicle tracks the vehicle dynamics in the motor-only driving mode. Hence, the target output of the plant is the transient output of the reference model, instead of a constant or predefined value, which is impractical for a running vehicle (Grewe et al., 2007; Rao and Hassan, 2004).

Figure 1 HDCT vehicle architecture (see online version for colours)

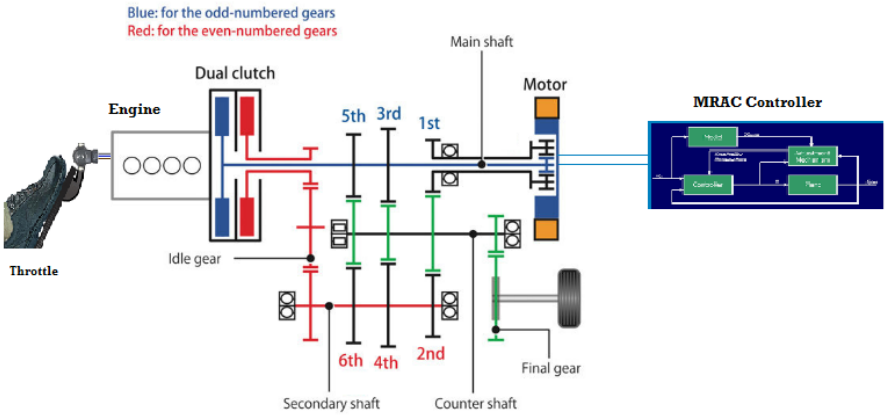

The model reference adaptive controller (MRAC) controller have been well established for many nonlinear problems, such as the Shunt active power-filter system (Shyu et al., 2008), the piezo-positioning system (Liu et al., 2010), the three-phase three level boost rectifier (Yacoubi et al., 2006), controlling water level of boiler system (Kadu et al., 2015), DC electric drive alone (Coman and Boldisor, 2013), and control and real-time optimisation of dry dual clutch transmission during the vehicle's launch (Zha et al., 2014). In addition, a model reference control law is proposed to coordinate the motor torque, engine torque, and clutch torque to manage transitions to series-parallel hybrid electric vehicle (SPHEVs) (Chen et al., 2012).

2 Statement of the problem

The mode transition from motor only to the combined mode or between other modes may cause disturbances to the output torque, leading to jerky motions and excessive wear to the clutch friction plates. Mode shifting has been a concern in hybrid vehicles with similar configurations.

The drivability and dynamics of HEVs especially during mode changes have drawn a lot of attention, and many researchers have recently studied dynamics and control during clutch engagement for conventional vehicles (Zhang et al., 2002; Crowther et al., 2004), their strategies and conclusions are not directly applicable to the problem at hand, given the differences between HDCT and conventional vehicles. For HDCT, one more external

torque, i.e., the motor torque, is applied to the powertrain, together with the engine torque. Others have applied the controller mechanism to SPHEV with conventional transmission only.

In Beck et al. (2005), model predictive control is applied for clutch engagement control in an HEV based on a simplified drivetrain model. In Koprubasi et al. (2007), a model-based stabilising controller is developed for the control of the engine and motor during mode transition. In Kim et al. (2009), the scheduling of the powertrain components, such as the clutch pressure, is applied to achieve smooth HEV mode changes. Accordingly, their control objectives are different. For HDCT, the engine and the traction motor are two alternative power sources, and thus, the objective is to smoothly engage the clutch without causing torque interruption, regardless of which source is powering the vehicle.

A similar design has been patented by GM with two electric machines (one as generator), but was never developed as a product. Our system is equipped with one motor that can serve as a generator as well; in this case, the design is less expensive and the torque range of the EM does not need to be high since the EM torque can be multiplied by the DCT. Figure 2 shows some similar designs equipped with one motor only. The first configuration (EM connected before transmission) and the third configuration (EM connected after transmission) are similar to the powertrain of the 'Audi A3-etron' and 'P1-McLaren' respectively, exhibited at the March 2013 Geneva Motor Show (Upendra, 2004). The second configuration (EM connected within transmission) is our design studied in this paper. As can be seen, the design in this paper is different from the existing ones.

Figure 2 Different parallel hybrid architectures (see online version for colours)

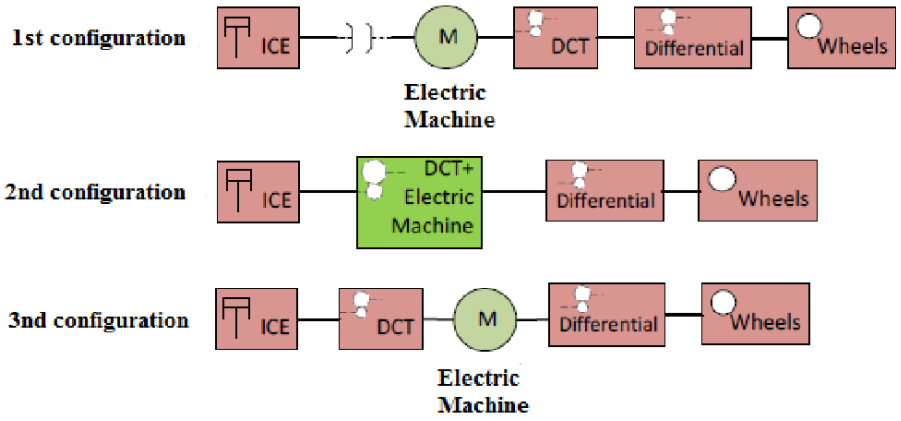

To the best of our knowledge, no relevant literature on MRAC with HDCT system (motor connected within transmission) problems have been found. This paper proposes a model reference adaptive control (MRAC) to achieve smooth transitions by covering the power lost by the engine, with reduced driveline interruption and frictional losses for HDCTs.

3 The equations for the dynamics

The dynamic equations of each subsystem are provided in this section.

3.1 The electric motor

The equations for the electric motor are

$$I_{\text{mot}}\frac{d\,\omega_{\text{mot}}}{dt} + b\,\omega_{\text{mot}} = Ki - T_{\text{mot}} \tag{1}$$

$$i = \frac{V_{dc} - \xi}{R}, \xi = K\omega_{\text{mot}}. \tag{2}$$

Eliminating i and ξ we get

$$I_{\text{mot}}\frac{d\,\omega_{\text{mot}}}{dt} + [b + \frac{K^2}{R}]\omega_{\text{mot}} = \frac{KV_{dc}}{R} - T_{\text{mot}}, \tag{3}$$

where I_{mot} is the effective inertia of the motor, i is the current in the armature circuit, T_{mot} is the torque delivered to the drive train by the motor, V_{dc} is the voltage supplied to the motor from the battery, b is the motor friction constant, K is the electromotive force constant; R is the resistance of armature circuit;and ω_{mot} is the motor speed in rad/s.

3.2 The internal combustion engine

The characteristics of an internal combustion engine (ICE) can be represented by a nonlinear static map. The torque generated by the engine depends on the fuelling (u_{ic}) and the engine speed (ω_{ic}). The engine is modelled as a function of the current throttle input from the driver pedal (fuel) and the engine speed as shown in Figure 3.

Figure 3 Engine fuel map as a function of throttle and engine speed (see online version for colours)

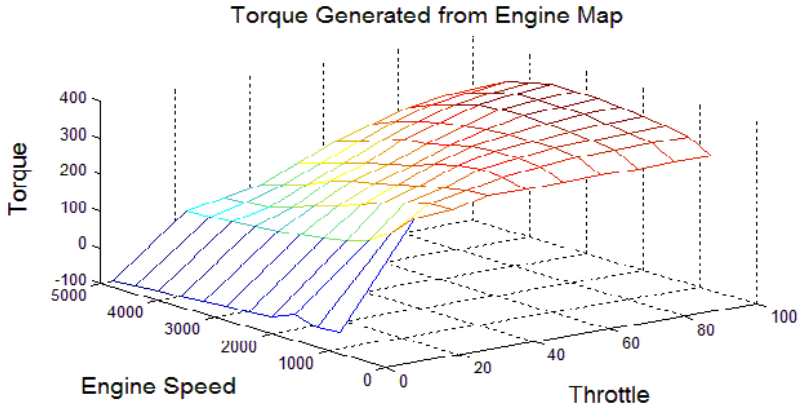

The engine torque can be expressed as,

$$T_{ic} = f(u_{ic}, \omega_{ic}),$$

where u_{ic} is the engine fuel input; ω_{ic} is the engine speed in rad/s.

We approximate $f(u_{ic}, \omega_{ic})$ by a quadratic function in u_{ic} and ω_{ic}, the resulting engine torque equation can be written as,

$$\begin{aligned} T_{ic} =&(c_{11}\omega_{ic}^2 + c_{12}\omega_{ic} + c_{13})u_{ic}^2 + (c_{21}\omega_{ic}^2 + c_{22}\omega_{ic} + c_{23})u_{ic} \\ &+(c_{31}\omega_{ic}^2 + c_{32}\omega_{ic} + c_{33}). \end{aligned} \tag{4}$$

C_{ij} (for i, j=1,2,3) are constant values derived for the approximation of the quadratic function of the fuel map using the Maxima tool. Figure 4 quantify the percentage change for fuel engine map and its approximation from quadratic function.

Applying Newton's second law, we obtain,

$$I_{ic}\frac{d\omega_{ic}}{dt} = T_i - T_{ic}, \tag{5}$$

where I_{ic} is the effective inertia of engine, T_i is the torque generated by the ICE, and T_{ic} is the torque delivered to the drive train.

Figure 4 Percentage change for fuel engine map and its approximation quadratic function (see online version for colours)

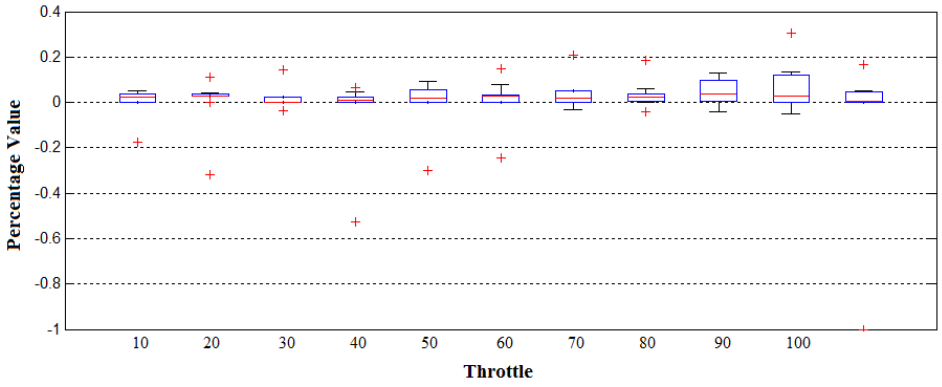

3.3 Dual clutch transmission

A DCT combines the convenience of an automatic transmission with the fuel efficiency of a manual transmission. It houses two separate clutches, one for odd and one for even gear sets, eliminating the need for a torque converter. To ensure smooth shifting and optimal efficiency, DCTs need sophisticated controllers capable of preselecting the next gear and engaging the appropriate clutch precisely when required.

The torque transmitted through DCT can be expressed as,

$$I_{\mathrm{DCT}}\frac{d\omega_{\mathrm{DCT}}}{dt} = T_i - T_{\mathrm{DCT}},$$

where T_{DCT} is the torque carried by DCT, ω_{DCT} and I_{DCT} are the speed and the mass moments of inertia of the flywheel, respectively.

For the sake of easily designing the controller, further assumptions about motional relationship among the output shafts of transmission and the engine speed should meet the equations $\omega_{ic} = \omega_{\mathrm{DCT}}$, $\omega_{\mathrm{mot}} = \omega_{ic}\,(i_{\mathrm{mot}}/i_{ic})$ and the gear imposes a single constraint, specified by the fixed gear ratio,consequently the DCT equation is embedded into the HDCT plant equation.Then the HDCT simplified model is shown in Figure 5.

Figure 5 Schematic of hybrid dual clutch transmission (see online version for colours)

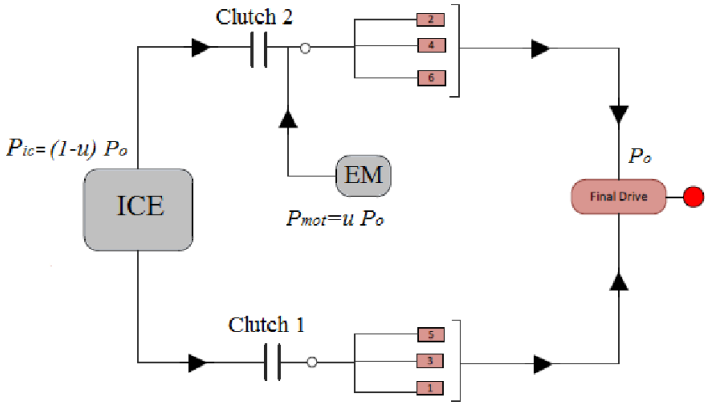

The power split ratio u for HDCT design is defined as the power request to the motor (P_{mot}) divided by the total power request at the wheels (P_o), which can be expressed as,

$$u = \frac{P_{\mathrm{mot}}}{p_o}.$$

Therefore,ICE torque and power are given by,

$$T_{ic} = \frac{(1-u)}{i_{ic}} T_o,\ P_{ic} = (1-u)P_o.$$

Motor torque and power are given by,

$$T_{\mathrm{mot}} = \frac{(u)}{i_{\mathrm{mot}}} T_o,\ P_{\mathrm{mot}} = uP_o.$$

3.4 The hybrid system of the motor, engine and DCT

Both the engine and the motor provide the required power to the drive shaft, depending on the vehicle speed. The vehicle torque output can be expressed as,

$$T_o = i_{\mathrm{mot}} T_{\mathrm{mot}} + i_{ic} T_{ic}. \tag{6}$$

where i_{mot} and i_{ic} are a constant ratio.

The longitudinal vehicle dynamics can be expressed as,

$$F_p = mg(f_0 + f_1 v) + mg\sin\theta + \frac{1}{2}\rho C_D A v^2, \tag{7}$$

where C_D is the aerodynamic drag coefficient, v is the vehicle speed, f_0 and f_1 are the friction force constants, and $mgsin\theta$ is the incline force.

Applying Newton's law yields,

$$m\frac{dv}{dt} = \frac{T_o}{r} - F_p \tag{8}$$

and the hybrid plant equation is,

$$\frac{dv}{dt} = C_0 + C_1 v + C_2 v^2 + BV_{dc}, \tag{9}$$

where C_0, C_1, C_2 and B can be expressed as,

$C_0 = \frac{r(c_{13} i_{ic} u_{ic}^2 + c_{23} i_{ic} u_{ic} - mg\, r \sin\theta - f_0\, mg\, r + c_{33} i_{ic})}{I_T}$,

$C_1 = -\frac{i_{\rm mot} I_T BK - c_{12} i_{ic}^2 r u_{ic}^2 - c_{22} i_{ic}^2 r u_{ic} + f_1 mg\, r^3 + b\, i_{\rm mot}^2 r - c_{32} i_{ic}^2 r}{I_T\, r}$,

$C_2 = -\frac{\frac{1}{2}\rho\, C_D r^3 A - c_{11} i_{ic}^3 u_{ic}^2 - c_{21} i_{ic}^3 u_{ic} - c_{31} i_{ic}^3}{I_T\, r}$,v $B = \frac{i_{\rm mot}\, rK}{I_T\, R}$,

$I_T = m\, r^2 + i_{\rm mot}^2\, I_{\rm mot} + i_{ic}^2\, I_{ic}$.

Following assumptions are made for equation (9):

- The slope of the road is assumed to be negligible.
- When the throttle is constant: C_0, C_1, C_2 and B are always constant parameters.
- When the throttle is varying, the parameters will vary slowly and the switching from one value to another occurs at low frequencies. In the throttle change case,there should be enough time between changes so that θ_t^* can guarantee closed-loop stability and the adaptive law has time to 'learn' about the change in the parameters, the same approach as above can be used to show that the error will be bounded, provided the switching frequency is sufficiently small, as shown in Figure 7.

The system described by equation (9) can be easily converted to the first order linear system using feedback linearisation. We are primarily interested in systems where v tracks a desired speed profile v_d, and it is slightly more intuitive to write the control law as,

$$V_{dc} = \theta_1 v_d + \theta_2 (v_d - v) + \theta_3 + \theta_4 v^2. \tag{10}$$

Note that the feedback law given in equation (10) can be written in a concise form as,

$$\mathbf{V_{dc}} = \begin{bmatrix}\theta_1 & \theta_2 & \theta_3 & \theta_4\end{bmatrix} \begin{bmatrix} v_d \\ v_d - v \\ 1 \\ v^2 \end{bmatrix} = \theta\, \Phi. \tag{11}$$

The choice of the symbols θ and Φ is to be consistent with the generally accepted notation used in MRAC, and θ is a vector of gains to be determined. The gains θ_i can be expressed as,

$$\theta_1 = \frac{(-C_1 - a_m + b_m)}{B}; \theta_2 = \frac{(C_1 + a_m)}{B}$$

$$\theta_3 = \frac{-C_0}{B}; \theta_4 = \frac{-C_2}{B}.$$

The above choice of gains will result in the following closed-loop system,

$$\frac{dv}{dt} = -a_m v + b_m v_d.$$

This shows that by proper choice of the gains, we can obtain any first order linear system behaviour.

In the next section, we briefly introduce the key results concerning the model reference adaptive control (MRAC) to show how we can design an adaptive control so that the gains can be tuned in real time to achieve any first order linear system behaviour.

Figure 6 The MRAC architecture for HDCT

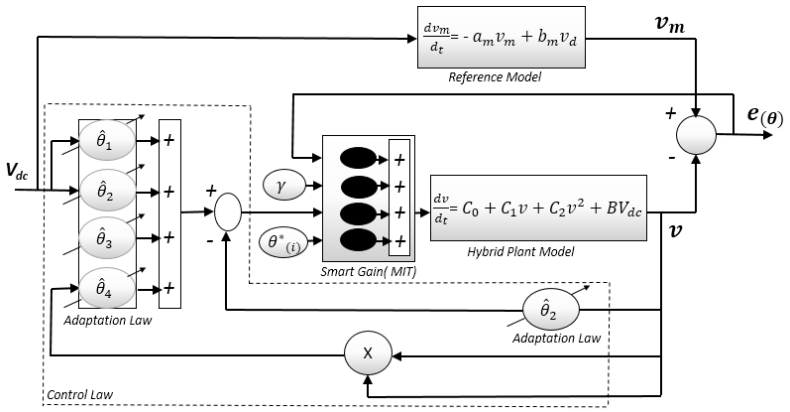

4 The adaptive control law

4.1 The MRAC architecture

The MRAC architecture (as shown in Figure 6) contains a reference model that is built to match the desired powertrain dynamics of the driving mode. An output feedback MRAC algorithm will be proposed, the conditions for closed-loop system stability will be derived, and the methods for selecting input combinations and controller parameters will be discussed. The discussions and experimental results presented will establish the effectiveness of the proposed MRAC.

4.2 The MIT rule

The gradient method, also referred as the MIT rule, was developed by the Instrumentation Laboratory at the Massachusetts Institute of Technology (MIT) (Landau et al., 2011). It will be assumed that in the closed-loop system, the controller has one adjustable parameter θ. The parameter $e(\theta)$ represents the error between the output of the plant ($y_{\text{plant}}(\theta)$) and the output of the model reference ($y_{\text{model}}(\theta)$). The goal here is to adjust θ to minimise the cost function $J(\theta) = \frac{1}{2}e^2(\theta)$ (Narendra and Valavani, 1978).

- The tracking error is: $\mathbf{e}(\theta) = y_{\text{plant}}(\theta) - y_{\text{model}}(\theta)$
- The form cost function is: $\mathbf{J}(\theta) = \frac{1}{2}e^2(\theta)$
- The update rule is: $\frac{d\theta}{dt} = -\gamma\frac{\delta J}{d\theta} = -\gamma e\frac{\delta e}{d\theta}$

It is important to highlight that change in θ is proportional to the negative gradient of $J(\theta)$.

4.3 The adaptive control law

The adaptive control law is very general. Here, we focus on a special case of a first order system where the model is a stable linear system (Ioannou and Fidan, 2006). The adaptation is a set of feedback gains, and the control signal given in (11) for the MIT rule can be expressed as,

$$\dot{\theta} = -\gamma\, \Phi^T\, e. \tag{12}$$

In terms of each gain, the above formula is decoupled and can be written as,

$$\dot{\theta_1} = -\gamma\, v_d\, e; \dot{\theta_2} = -\gamma\, (v_d - v)\, e; \dot{\theta_3} = -\gamma\, 1\, e; \dot{\theta_4} = -\gamma\, v^2\, e.$$

5 Proving the control law and stability using Lyapunov's Method (Elzaghir et al., 2017)

The adaptive control of non-linear plants using the MRAC method is discussed next. The hybrid system developed from the complex system can be represented using the following first-order differential equation,

$$\frac{dv}{dt} = C_0 + C_1 v + C_2 v^2 + BV_{dc}. \tag{13}$$

where v and V_{dc} represent plant output and input, respectively, and v^2 denotes the quadratic engine map.

5.1 Problem specification

Let the desired performance of the adaptive control system be specified by a first-order reference model,

$$\frac{dv_m}{dt} = -a_m v_m + b_m v_d. \tag{14}$$

where a_m and b_m are constant parameters and v_d is a bounded external reference signal. The parameter a_m is required to be strictly positive to ensure the stability of the reference model, and b_m is chosen to be strictly positive without loss of generality (Narendra and Valavani, 1978). The motivation behind using the adaptive control design is to formulate a control law and an adaptation law such that the resulting error $v - v_m$ asymptotically converges to zero.

5.2 Choice of control law

As the first step in the adaptive controller design, let us choose the control law to be,

$$\mathbf{V_{dc}} = \hat{\theta}_1 v_d + \hat{\theta}_2 (v_d - v) + \hat{\theta}_3 + \hat{\theta}_4 v^2. \tag{15}$$

where $\hat{\theta}_1$, $\hat{\theta}_2$, $\hat{\theta}_3$, and $\hat{\theta}_4$ are variable feedback gains. With this control law, the closed-loop dynamics can be expressed as,

$$\frac{dv}{dt} = (C_1 - B\hat{\theta}_2)v + (B\hat{\theta}_1 + B\hat{\theta}_2)v_d + B\hat{\theta}_3 + C_0 + (B\hat{\theta}_4 + C_2)v^2. \tag{16}$$

If the plant parameters were known, the values of the control parameters would be (initial values),

$$\theta_1^* = \frac{(-C_1 - a_m + b_m)}{B};\ \theta_2^* = \frac{(C_1 + a_m)}{B}$$

$$\theta_3^* = \frac{-C_0}{B};\ \theta_4^* = \frac{-C_2}{B}$$

which would lead to closed-loop dynamics identical to the reference model dynamics, and yield zero tracking error. In this case, the first term in equation (15) would result in the right DC gain, while the second term in the control law equation (15) would achieve the dual objectives of cancelling the term $C_1\, v$ in equation (13) and imposing the desired pole $a_m\, v_m$.

In the adaptive control problem, since C_0 C_1, C_2 and B are unknown, the control input will achieve these objectives adaptively, i.e., the adaptation law will continuously search for the right gains, based on the tracking error $v - v_m$, so as to make v tend to v_m asymptotically.

5.3 Choice of adaptation law

The adaptation law for the parameters $\hat{\theta}_1$, $\hat{\theta}_2$, $\hat{\theta}_3$ and $\hat{\theta}_4$ can be chosen as follows.

Let,

$$e = v - v_m, \tag{17}$$

be the tracking error. The error of each parameter is defined as the difference between the controller parameter provided by the adaptation law and its corresponding ideal parameter, i.e.,

$$\tilde{\theta}(\mathbf{t}) = \begin{bmatrix} \tilde{\theta}_1 \\ \tilde{\theta}_2 \\ \tilde{\theta}_3 \\ \tilde{\theta}_4 \end{bmatrix} = \begin{bmatrix} \hat{\theta}_1 - \theta_1^* \\ \hat{\theta}_2 - \theta_2^* \\ \hat{\theta}_3 - \theta_3^* \\ \hat{\theta}_4 - \theta_4^* \end{bmatrix}. \tag{18}$$

The dynamics of the tracking error can be found by subtracting equation (16) from equation (14) results in,

$$\frac{de}{dt} = \frac{dv}{dt} - \frac{dv_m}{dt}$$

$$\begin{aligned} \frac{de}{dt} = (C_1 - B\hat{\theta}_2)v + (B\hat{\theta}_1 + B\hat{\theta}_2)v_d + B\hat{\theta}_3 + C_0 + \\ (B\hat{\theta}_4 + C_2)v^2 + a_m v_m - b_m v_d. \end{aligned} \tag{19}$$

Thus, the adaptation law can be expressed as,

$$\dot{\hat{\theta}}_1 = -\gamma\, e\, v_d; \quad \dot{\hat{\theta}}_2 = -\gamma\, e\, (v_d - v); \quad \dot{\hat{\theta}}_3 = -\gamma\, e; \quad \dot{\hat{\theta}}_4 = -\gamma\, e\, v^2.$$

5.4 Tracking convergence analysis

With the control law and adaptation law chosen above, we can now analyse the system's stability and convergence behaviour using Lyapunov theory. The Lyapunov candidate function can be expressed as,

$$\begin{aligned} V = \frac{1}{2}e^2 + \frac{B}{2\gamma}(\hat{\theta}_1 - \theta_1^*)^2 + \frac{B}{2\gamma}(\hat{\theta}_2 - \theta_2^*)^2 + \\ \frac{B}{2\gamma}(\hat{\theta}_3 - \theta_3^*)^2 + \frac{B}{2\gamma}(\hat{\theta}_4 - \theta_4^*)^2. \end{aligned} \tag{20}$$

It is important to note that the error goes to zero if the parameters of the controller are set to the initial values. This function is zero only when the error is zero and the controller parameters have the correct values. The derivative of V is given as,

$$\begin{aligned} \frac{dV}{dt} = \frac{de}{dt}e + \frac{B}{\gamma}(\hat{\theta}_1 - \theta_1^*)\dot{\hat{\theta}}_1 + \frac{B}{\gamma}(\hat{\theta}_2 - \theta_2^*)\dot{\hat{\theta}}_2 + \\ \frac{B}{\gamma}(\hat{\theta}_3 - \theta_3^*)\dot{\hat{\theta}}_3 + \frac{B}{\gamma}(\hat{\theta}_4 - \theta_4^*)\dot{\hat{\theta}}_4. \end{aligned} \tag{21}$$

Substituting equation (19) into equation (21) with the values

$$a_m = -C_1 + B\theta_2^*;\ b_m = B(\theta_1^* + \theta_2^*)\Delta\theta_x = \hat{\theta}_x - \theta_x^*$$

yields

$$\begin{aligned}\frac{dV}{dt} &= e[C_1 v - B\hat{\theta}_2 v + B\hat{\theta}_1 v_d + B\hat{\theta}_2 v_d + B\hat{\theta}_3 + \\ &(B\hat{\theta}_4)v^2 - C_0 - C_2 + a_m v_m - B\theta_1^* v_d - B\theta_2^* v_d] \\ &+\frac{B}{\gamma}(\Delta\theta_1)(-\gamma\, e\, v_d) + \frac{B}{\gamma}(\Delta\theta_2)(-\gamma\, e\,(v_d - v)) \\ &+\frac{B}{\gamma}(\Delta\theta_3)(-\gamma\, e) + \frac{B}{\gamma}(\Delta\theta_4)(-\gamma\, e\, v^2).\end{aligned} \tag{22}$$

If the parameters are updated as

$$\dot{\hat{\theta}}_1 = -\gamma\, e\, v_d;\quad \dot{\hat{\theta}}_2 = -\gamma\, e\,(v_d - v);\quad \dot{\hat{\theta}}_3 = -\gamma\, e;\quad \dot{\hat{\theta}}_4 = -\gamma\, e\, v^2. \tag{23}$$

The resulting derivative of the Lyapunov candidate function can be expressed as,

$$\frac{dV}{dt} = -a_m(v - v_m)e. \tag{24}$$

and

$$e = v - v_m$$

and therefore the final result is given as,

$$\frac{dV}{dt} = -a_m e^2.$$

Thus, the adaptive control system is globally stable, i.e., the signals e, $\hat{\theta}_1$, $\hat{\theta}_2$, $\hat{\theta}_3$ and $\hat{\theta}_4$ are bounded. Furthermore, the tracking error ($e(t)$) is guaranteed to be asymptotically convergent to zero because the boundedness of e, θ_1^*, θ_2^*, θ_3^* and θ_4^* implies the boundedness of $e(t)$, which implies the uniform continuity of V.

As a result, the error function will converge to zero, for the adaptive control system is globally stable. A short analysis of Figure 7 reveals the powerful development of the control system and demonstrates its adjustability.

6 Results and discussion

Hybrid vehicles can change modes in many ways, and the selection of mode is dependent on various parameters, such as pressing the accelerator pedal, the state of charge (SOC) of the battery pack, the current vehicle speed, the torque required by the driver, the minimum value of SOC of the battery pack, the maximum permissible motor torque, the maximum vehicle speed in motor only mode, etc. The parameters are checked for determining the correct operating mode of the vehicle. If the parameter condition is satisfied, then the next parameter is checked, until a particular mode is decided on. This section includes three parts:

- the interaction between various modes
- sensitivity and performance of the MRAC during the mode transition
- a simulation study to compare the results of the proposed MRAC and conventional operation.

Figure 7 Error function converges to zero (see online version for colours)

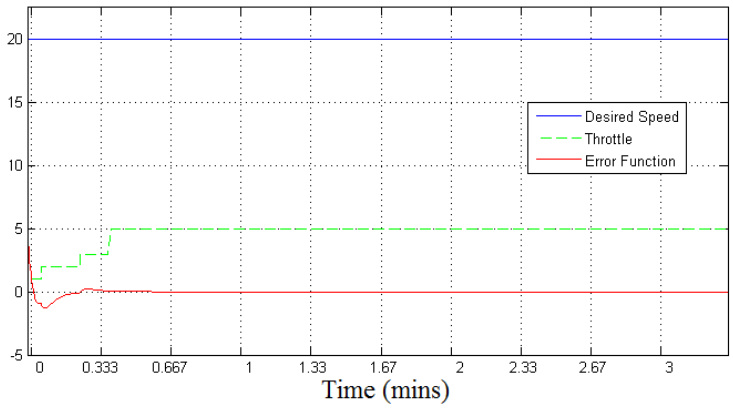

6.1 Interaction between various modes

Mode interactions are important elements of the control logic as they are the special conditions when the system goes from one mode directly to an other mode: they are the factors that contribute to the response of the MRAC control system. The proposed system has five operating modes when the vehicle is in motion and one operating mode for standstill charging operation.

- *Motor alone mode*: The vehicle is always launched in the motor only mode. The vehicle operates in this mode up to a maximum speed defined by the controller, provided that the SOC is greater than the minimum SOC for the battery (as per the system design). Since the engine does not operate in this mode, the dual clutches are disengaged, to prevent any backlash to the engine.
- *Combined mode*: This mode is selected when high torque is required for situations such as sudden acceleration or climbing a grade. This mode is also selected if the vehicle speed becomes greater than the maximum speed defined by the controller in the motor alone mode. Both the engine and the motor provide propulsive power to the drive shaft.
- *Engine alone mode*: This mode involves the engine as the only source of propulsion. The engine transmits power to a lowest possible gear ratio such that the engine remains in the best efficiency window.
- *Regenerative braking mode*: The motor is coupled to the output shaft through gears and it can function as a generator as well. This is used to recover the energy that is consumed in braking to charge the battery.

- *Brake mode*: This is a special operating condition when the battery SOC is more than the maximum SOC limit and a braking operation is required. The controller operates only the conventional brakes in this mode. No power is regenerated from the drive shaft.

The diagram in Figure 8 shows the interaction of various vehicle powertrain modes. For example, if the vehicle is in regenerative mode and if it still decelerates, but the SOC is already charged up to the maximum SOC, then the controller changes the mode to mechanical brake mode. Similarly, if the vehicle's required speed increases above the speed threshold of the motor, the mode changes from motor-alone mode to combined mode. In this mode, the vehicle is driven by both the motor and the engine.

Figure 8 Interaction between various modes (see online version for colours)

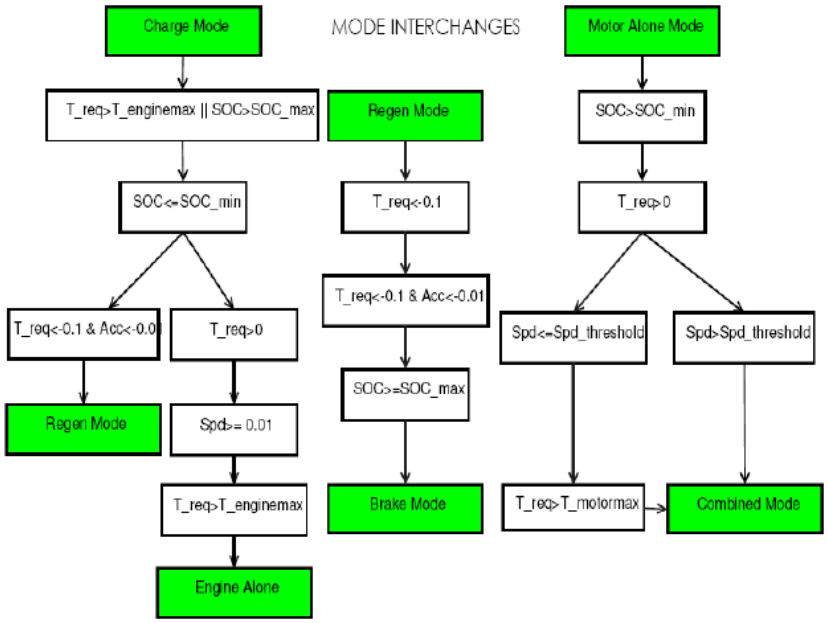

6.2 *Sensitivity analysis*

To further understand the design implications of the MRAC strategy, we considered the key factors that influence the mode transition performance, including the three learning variables $\gamma 1$, $\gamma 2$ and $\gamma 3$ in Table 1.

The selection of γ in the update rule will determine the behaviour of the MRAC for motor torque response. One example of γ is given in Figure 9. The MRAC mode transition control yields good performance for the three different values. The results for different predefined values of γ are not similar. Therefore, we conclude that the performance of the proposed MRAC is sensitive to different learning rate values.

Table 1 Gamma values for the control law signals

Parameters	*Values*
$\gamma 1$	$10e^{-}2$
$\gamma 2$	$10e^{-}3$
$\gamma 3$	$10e^{-}4$

The three different values of γ are used in simulation to assess the sensitivity of the performance to this design parameter.

- A larger value of γ ($\gamma 1$ or higher) leads to a torque disturbance, see the final stage in the process of Figure 9 at time 28–30 s.
- Choosing smaller γ is helpful for reducing the disturbance. Moreover, a small γ (such as $\gamma 2$ or $\gamma 3$) allows for shorter times for the MRAC to compensate for the torque losses. Consequently, a large γ in those cases causes an intensive vehicle jerk at mode transition. Thus, a small γ is usually used in real applications to avoid this problem.

For this reason, most of the simulations presented in this paper use a small γ since the MRAC, in this case, prevents a disturbance or a sudden jerk, and provides shorter time responses.

Figure 9 MRAC responses to different γ values (see online version for colours)

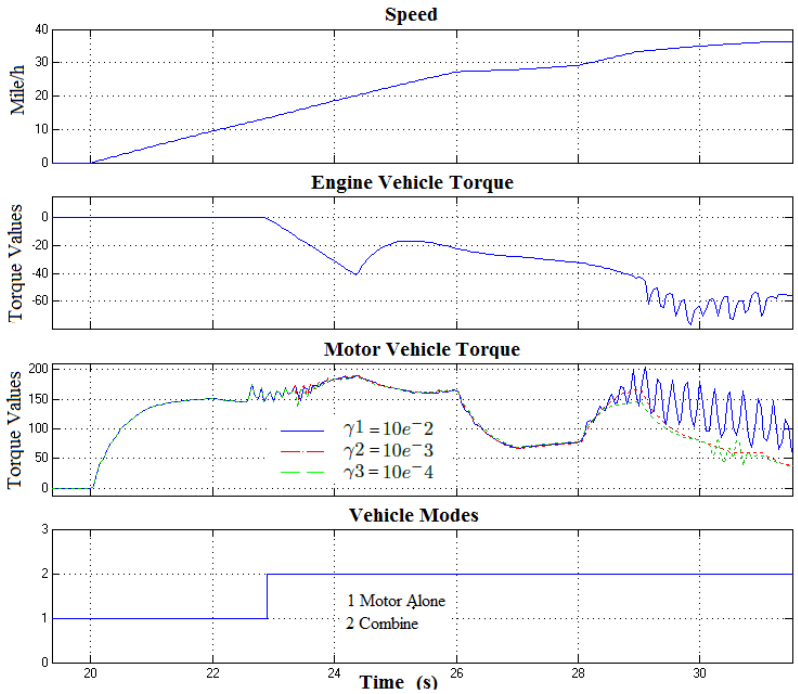

6.3 Driving selection modes

Our first experiment has the following aims:

- *Comfortable car*:

This mode has smooth shifting with no sense of any gear change, therefore, it takes longer to reach the desired value, as shown in Figure 10.

$$\text{Desired Model}: \quad \frac{dv}{dt} = -0.1(v_d - v).$$

- *Sporty shifting car*:

This mode allows the driver to feel the shifting of the transmission and have the manual transmission experience; it takes less time to reach the desired value, as shown in Figure 11.

$$\text{Desired Model}: \quad \frac{dv}{dt} = -10(v_d - v).$$

Figure 10 Response of the comfortable car (see online version for colours)

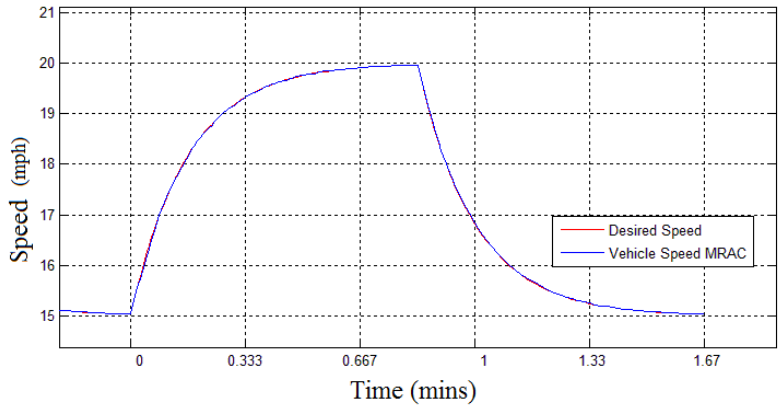

6.4 Sensitivity of the MRAC when changing modes

The MRAC will step up and supply more voltage to the motor during mode changes to deliver higher torque in order to cover the power lost by the engine for smooth shifting and balancing.

- Figure 12 shows the graphs for various parameters in the HDCT model. The graphs provide a correlation between the vehicle speed, controller mode, and vehicle torque. It can clearly be seen that since the torque demand of the drive cycle can be met by just the motor, the controller always selects the motor-only mode (1). The engine cranks in at around 23 s when the controller mode changes from motor-alone mode (1) to combined mode (2) since the motor cannot provide the required torque and the

MRAC compensates for the power lost in the system within that transition (from time 23 s to 25 s). Similarly for Figure 13: the MRAC controller switches to combined mode (2) when we have speed deceleration; On the other hand, when the driver is accelerating with a speed exceeding 40, the controller changes from motor-alone mode (1) to engine only mode (3) since the motor cannot provide the required torque as the battery SOC is low (Figure 14).

- In the case of deceleration, the controller selects mode 5 (regenerative mode) as can be seen in Figure 15. It also exemplifies the control strategy that prevents the SOC from going below minimum limit (0.4 in this test case).
- For HWY drive cycle and with the SOC being higher than the lower limit set by the design (0.4), the controller selects brake mode in the event of continued vehicle deceleration and uses the extra power to charge the battery if needed (Figure 16).

The simulation shows the various torque inputs and outputs for the propulsion elements, namely the engine and the motor. It can be seen that both propulsion system elements follow the command set by the controller, indicating that each subsystem's (engine and motor) controllers are controlling correctly. It also gives an understanding of the split that the controller decides on in order to meet a torque demand.

Figure 11 Response of the sporty car (see online version for colours)

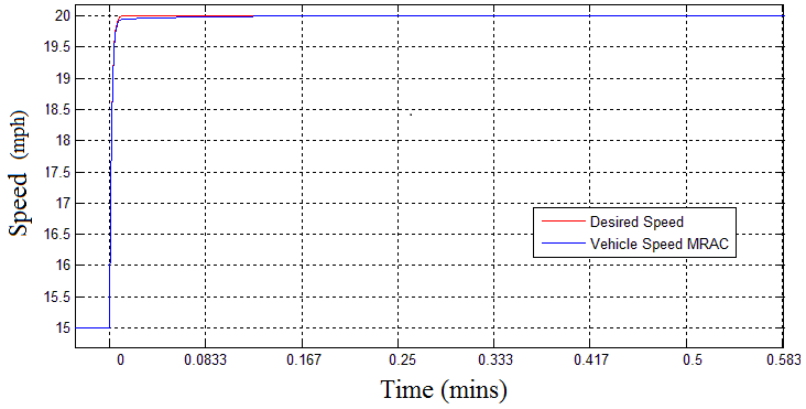

6.5 Comparison with the conventional method

To compare the performance of the two-mode transition strategies, we consider the scenario of a typical startup process of the HDCT bus. The desired vehicle acceleration is positive. The results of the proposed MRAC and the conventional operation (abbreviated by Conv.) are discussed below.

The response of the MRAC is faster than that of the Conv., as shown in Figure 17. The MRAC controller is actuated earlier and with much higher intensity, so it quickly reacts to the startup and the MRAC controller will supply more voltage to the motor to run the vehicle. The mode transition begins at time 25 s when the mode changes from motor-alone to combined. The MRAC motor has boosted more torque to compensate for torque deficits

by the HDCT when the mode is changing to maintain balance. However, the Conv. falls before start responds slowly and stays in the low torque value.

Figure 12 Change from motor-alone mode to combined mode (see online version for colours)

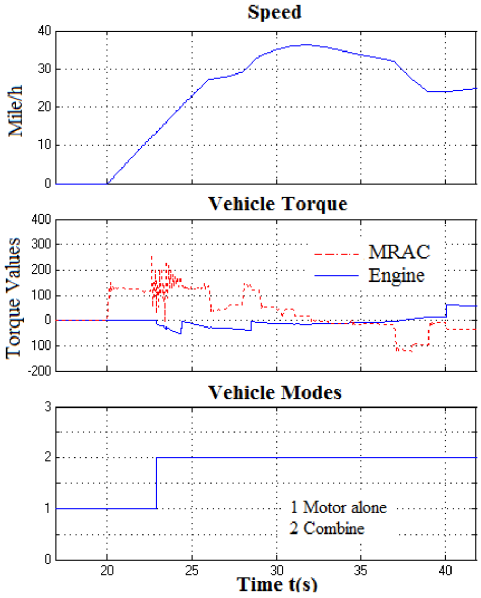

Figure 13 Change from combined mode to motor-alone mode (see online version for colours)

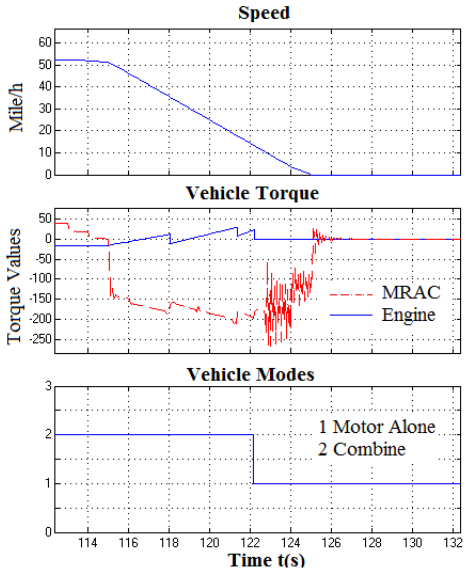

Figure 14 Change from motor-alone mode to engine mode (see online version for colours)

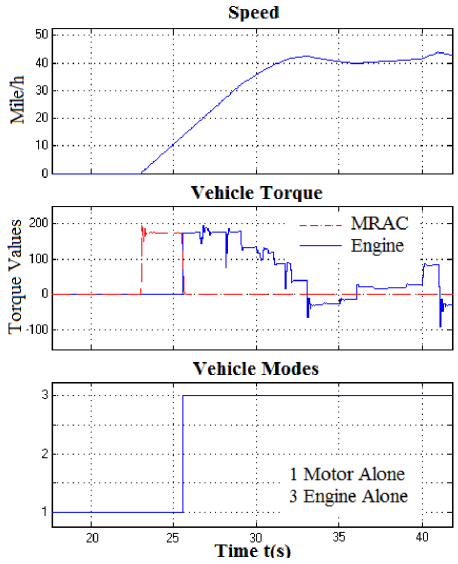

Figure 15 Change from combined mode to Regen (see online version for colours)

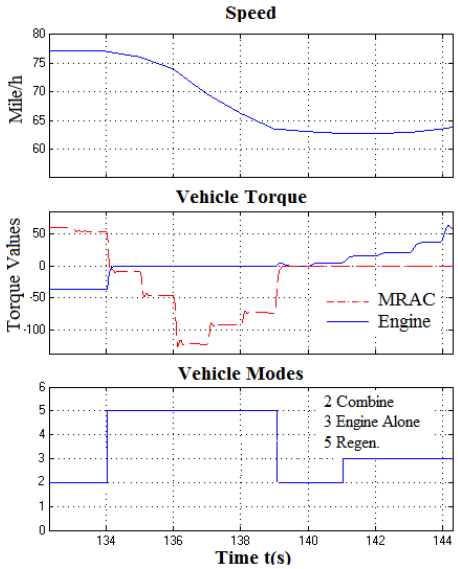

As shown at time 122 s in Figure 18, when the mode is switching from combined to motor-alone, the MRAC controller responds quickly to the transition and produces extra torque as a result of the fast response by the motor to compensate for the disengagement of the engine. The vehicle acceleration of the MRAC is maintained in a good balance at time 162 s, whereas that of the Conv. falls by 100 points at the end of the phase. For the Conv., the

profile of the vehicle acceleration is similar to that of the MRAC, which implies that both controllers respond correctly to the transitions. Moreover, the motor torque compensates for any torque changes in the system. However, the MRAC responds quickly.

Figure 16 Change from braking to engine mode (see online version for colours)

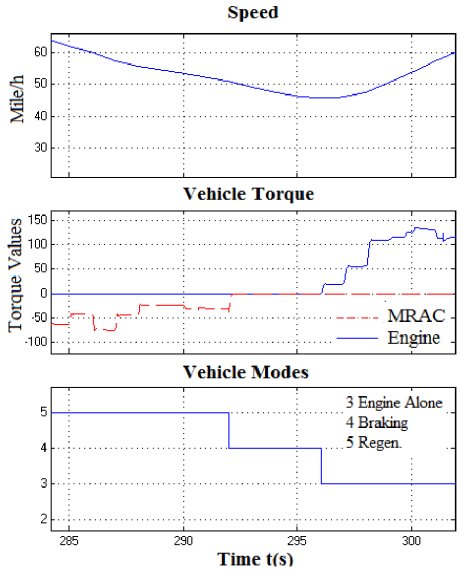

Figure 17 Conv. and MRAC responses during startup (see online version for colours)

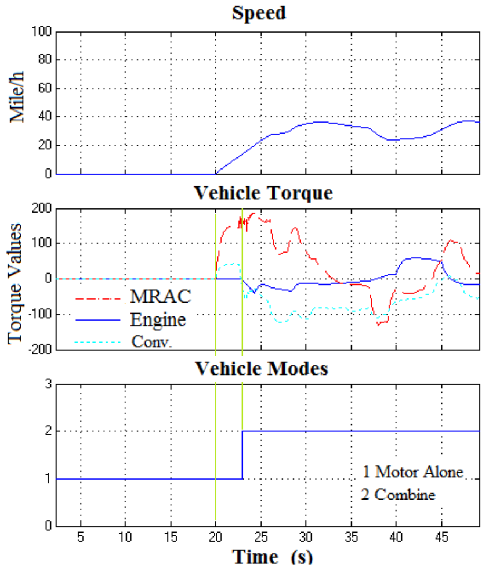

Figure 18 Conv. vs. MRAC responses during mode changes (see online version for colours)

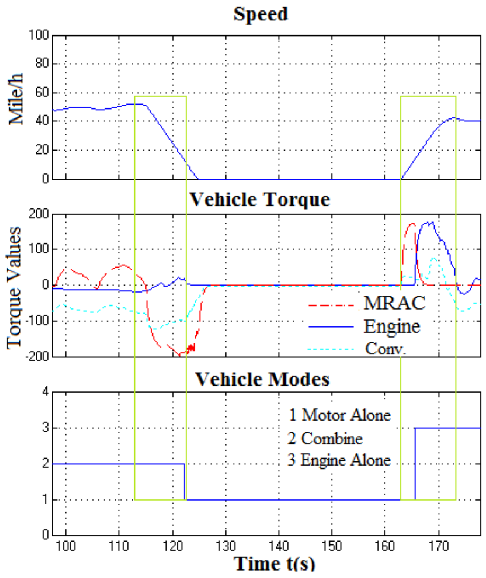

The reason for the sudden jerk is that Conv. cannot react quickly enough to the changes: the Conv.-controlled motor is clearly slower than the MRAC-controlled system. Finally, the performance of the Conv. controller quickly deteriorates, whereas the performance of the MRAC controller remains good. Obviously, the MRAC controller can considerably improve the behaviour of the motor in terms of this criterion.

It can be concluded that the HDCT design is more efficient than the conventional design in all conditions. Although the HDCT design improves the efficiency of the motor in compensating for all power lost in the system, it deteriorates the overall efficiency of the powertrain itself. This is mainly because of the inherent losses in the engine's architectural design during gear changes, because no motor loss is encountered when the power demand at the wheel is met by an ICE alone via the mechanical path.

7 Conclusions

In this paper, a model reference adaptive control (MRAC) has been designed to coordinate the motor torque and engine torque during mode transition for a hybrid vehicle with dual clutch transmission (HDCT). A dynamic model has been developed for the MRAC design, and a model-based analysis has been performed to derive the stability of a closed-loop system in the sense of Lyapunov. The MRAC takes the driving vehicle as the reference model, and the controller acts on the output errors between the reference model and the vehicle as the feedback signals to achieve smooth and efficient performance.

Several factors that can influence the performance of the MRAC mode transition have been studied through simulations. The proposed MRAC has yielded good performance for different values of the model's learning parameter for the update rule γ, which implies that the MRAC is adaptive to different torque distribution strategies. The MRAC method is applied to the mode transition of an HDCT bus. The simulation results confirm that

the MRAC outperforms the conventional operation method for an HDCT by reducing the vehicle jerk and the torque interruption for the driveline. Therefore, this paper shows that the MRAC is very promising. These promising results, particularly the experimental validation, have motivated us to further pursue the idea of MRAC and seek its robust and effective implementation of other mode transition control problems on other hybrid vehicle platforms.

References

Beck, R., Saenger, S., Richert, F., Bollig, A., Nei, K., Scholt, T., Noreikat, K.E. and Abel, D. (2005) 'Model predictive control of a parallel hybrid vehicle drivetrain', *Decision and Control, 2005 European Control Conference. CDC-ECC '05. 44th IEEE Conference*, 12–15 December, Seville, Spain, Vol. 12, No. 15, pp.2670–2675.

Chen, L., Xi, G. and Sun, J. (2012) 'Torque coordination control during mode transition for a series-parallel hybrid electric vehicle', *IEEE Transactions on Vehicular Technology*, Vol. 61, No. 7, September, pp.2936–2949.

Coman, S. and Boldisor, C. (2013) 'Model reference adaptive control For a DC electric drive', *Bulletin of the Transilvania University of BraÃ…ÂŸov Series I: Engineering Sciences*, Vol. 6(55), No. 2, pp.33–38.

Conlon, B. (2005) *Comparative Analysis of Single and Combined Hybrid Electrically Variable Transmission Operating Modes*, SAE Paper 2005-01-1162, 11 April.

Crowther, A., Zhang, N., Liu, D.K. and Jeyakumaran, J.K. (2004) 'Analysis and simulation of clutch engagement judder and stick-slip in automotive powertrain systems', *Proc. Inst. Mech. Eng., Part D-J. Autom. Eng.*, Vol. 218, No. 12, December, pp.1427–1446.

Elzaghir, W., Zhang, Y., Natarajan, N., Massey, F. and Mi, C. (2017) 'Model reference adaptive control for hybrid electric vehicle with dual clutch transmission configurations', *IEEE Transactions on Vehicular Technology*, Vol. PP, No. 99.

Grewe, T.M., Conlon, B.M. and Holmes, A.G. (2007) *Defining the General Motor 2-Mode Hybrid Transmission*,ž SAE Paper 2007-01-0273, 2007 SAE World Congress.

Ioannou, P. and Fidan, B. (2006) *Adaptive Control Tutorial. Volume 11 of Advances in Design and Control*, Society for Industrial and Applied Mathematics, Philadelphia, PA.

Kadu, C.B., Parvat, B.J. and Parekar, N.N. (2015) 'Modified MRAC for controlling water level of boiler system', *2015 International Conference on Computational Intelligence and Communication Networks (CICN)*, Jabalpur, India, pp.1537–1539.

Kim, S., Park, J., Hong, J. and Lee, M. (2009) *Transient Control Strategy of Hybrid Electric Vehicle during Mode Change*, SAE2009-01-0228, 20 April.

Koprubasi, K., Westervelt, E.R. and Rizzoni, G. (2007) 'Toward the systematic design of controllers for smooth hybrid electric vehicle mode changes', *Proceedings of the 2007 American Control Conference*, 9–13 July, New York City, USA, pp.2985–2990.

Landau, I.D., Lozano, R., M'Saad, M. and Karimi, A. (2011) *Adaptive Control: Algorithms, Analysis and Applications*, Springer-Verlag, London.

Liu, Y.T., Chang, K.M. and Li, W.Z. (2010) 'Model reference adaptive control for a piezo-positioning system', *Precision Eng.*, Vol. 34, No. 1, p.6269.

Narendra, K.S. and Valavani, L.S. (1978) 'Stable adaptive controller design direct control', *IEEE Trans. Auto. Control*, Vol. 23, August, pp.570–583.

Rao, M.P.R.V. and Hassan, A. (2004) 'New adaptive laws for model reference adaptive control using a non-quadratic Lyapunov function', *Proceedings of the 12th IEEE Mediterranean Electromechanical Conference*, Dubrovnik, Croatia, 1–15 May, pp.371–374.

Shyu, K.K., Yang, M.J., Chen, Y.M. and Lin, Y-F. (2008) 'Model reference adaptive control design for a shunt active-power-filter system', *IEEE Trans. Ind. Electron.*, Vol. 55, No. 1, January, p.97106.

Upendra, K. (2004) *Dual Clutch Transmission for Plug-in Hybrid Electric Vehicle Comparative Analysis with Toyota Hybrid System*, Chalmers University of Technology, Master's Thesis.

Waltermann, P. (1996) 'Modeling and control of the longitudinal and lateral dynamics of a series hybrid vehicle', *Proceedings of the 1996 IEEE International Conference*, Dearborn, MI, 15–18 September, pp.191–198.

Yacoubi, L., Ai-Haddad, K., Dessaint, L-A. and Fnaiech, F. (2006) 'Linear and nonlinear control techniques for a three-phase three-level NPC boost rectifier', *IEEE Trans. Ind. Electron.*, Vol. 53, December, pp.1908–1918.

Zhao, Z., Chen, H. and Wang, Q. (2014) 'Control and real-time optimization of dry dual clutch transmission during the vehicle's launch', *Hindawi Publishing Corporation*, Vol. 2014, Article ID 494731, 18 pages Published 2 February 2014.

Zhang, J., Chen, L. and Xi, G. (2002) 'System dynamic modelling and adaptive optimal control for automatic clutch engagement of vehicles', *Proc. Inst. Mech. Eng., Part D-J. Autom. Eng.*, Vol. 216, No. 12, December, pp.983–991.